

Emergence of Intricate Dynamical Response by Supercritical Parametrically Driven or Ringwise Coupled Subcritical Hopf Oscillators

Yoko Uwate †‡, Stefan Martignoli †, Yoshifumi Nishio ‡ and Ruedi Stoop †

†Institute of Neuroinformatics, UZH / ETH Zurich
 Winterthurerstrasse 190, 8057 Zurich, Switzerland
 Email: {yu001, mstefan, ruedi}@ini.phys.ethz.ch

‡Dept. of Electrical and Electronics Engineering, Tokushima University
 2-1 Minami-Josanjima, Tokushima, Japan
 Email: {uwate, nishio}@ee.tokushima-u.ac.jp

Abstract—The mammalian cochlea has impressive signal detection capabilities, due to active amplification processes, which originate in the cochlea's hair cells. In past research, a biomorphic cochlea model was designed that successfully incorporates these properties. In this study, we investigate the complicated behavior that a stable Hopf-type limit cycle generates if it is driven by an input signal and, in addition, its bifurcation parameter is parametrically modulated ($\mu(t) > 0$). In this rather natural setting, we have an interaction among the frequencies ω_0 (the natural frequency of the oscillator), ω (the frequency of the input signal) and ω_μ (the frequency of the parametrical modulation of μ). By using computer simulations, we demonstrate that through this nonlinear interaction, the form of the typical attractors undergo various unexpected qualitative changes.

I. INTRODUCTION

Recently, detailed studies of the human sensory systems have been performed on various levels. On the auditory domain, a focus has been to investigate how the cochlea operates in the human ear. In order to better understand this process, models of different complexities of the cochlea have been designed and their salient properties have been extracted [1]-[6]. Various experiments revealed that the outer hair cells (OHC), which reside on top of the basilar membrane, are the source of an active amplification (see [7]). However, this basic model put forward in [7] matches poorly with realistic cochlea responses. In our previous research, a biomorphic cochlea model was developed based on the Hopf differential equation, and it was confirmed that this model is able to reproduce the measured basilar membrane response with great precision [8]. However, we believe that many important advantages of the Hopf cochlea model are still veiled. In particular, we expect that nonlinear phenomena emerging from more involved situations than the basic set-ups investigated so far, may play an important role for the explanation of the superb signal-processing abilities of the mammalian cochlea.

In this study, we investigate the situation when a stable Hopf-type limit cycle is driven by an input signal and, in addition, its bifurcation parameter is parametrically modulated

($\mu(t) > 0$). By using computer simulations, we demonstrate that through the nonlinear interaction among the different oscillatory ingredients, we obtain various unexpected qualitative changes of the forms of the typical attractors.

II. CIRCUIT EQUATION

Consider the Hopf differential equation of oscillator model

$$\dot{z} = (\mu + i\omega_0)z - |z|^2z + Fe^{i\omega t}, \quad (1)$$

where the last term describes an external periodic forcing of frequency ω and where $z(t) \in \mathbb{C}$. ω_0 is the natural frequency of the oscillation, and $\mu \in \mathbb{R}$ assumes in what follows the role of a control parameter. If we choose $F = 0$ (no external driving), Eq (1) corresponds to the generic differential equation of a system displaying a Hopf bifurcation. For $\mu < 0$, the solution $z(t) = 0$ is a stable fixed point, while for positive μ , the fixed point solution becomes unstable and a stable limit cycle appears.

In past studies [9], the circuit model of the Hopf oscillator were derived and used for an electronic implementation of the circuit:

$$\begin{aligned} \dot{x} &= -\frac{A_\mu \tilde{\mu} \tilde{x}}{MCR_\mu} - \frac{A_f \tilde{p}}{A_z CR_f} - \frac{\tilde{y}}{CR_\omega} - \frac{A_z^2 (\tilde{x}^2 + \tilde{y}^2) \tilde{x}}{2M^2 CR_\gamma} \\ \dot{y} &= -\frac{A_\mu \tilde{\mu} \tilde{y}}{MCR_\mu} - \frac{A_f \tilde{p}}{A_z CR_f} + \frac{\tilde{x}}{CR_\omega} - \frac{A_z^2 (\tilde{x}^2 + \tilde{y}^2) \tilde{y}}{2M^2 CR_\gamma}. \end{aligned} \quad (2)$$

III. MODULATING THE HOPF PARAMETER $\tilde{\mu}$

The control parameter $\tilde{\mu}$ is essential for the operating Hopf cochlea. In this study, we consider the case that the control parameter $\tilde{\mu}$ is changed periodically. Figure 1 shows the modulation of $\tilde{\mu}$, where the horizontal axis is time and the vertical axis the value of $\tilde{\mu}$. In the following, we will denote the frequency of the modulated parameter $\tilde{\mu}$ by ω_μ , and the amplitude of $\tilde{\mu}$ by A .

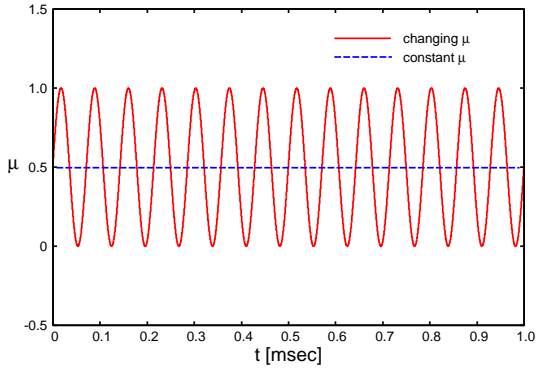


Fig. 1. Constant (dashed) and modulated (full line) parameter $\bar{\mu}$ vs time t .

IV. SIMULATED RESULTS

For simplicity, we first concentrate on the influence of the parametrical modulation of $\bar{\mu}$ alone. For our simulations, we choose the parameter of the oscillator model as follows. The center frequency of the Hopf oscillator $\omega_0/(2\pi) = 3.1$ [kHz], the amplitude of the input force $f = 0.1$, $A_\mu=10.0$, $A_f=10.0$, and $A_z=10.0$. Choosing $C=1\mu\text{F}$ yields the values $R_\omega=51.2\text{k}\Omega$, $R_\mu=51.2\text{k}\Omega$, $R_f=51.2\text{k}\Omega$ and $R_\gamma = 25.6\text{k}\Omega$ for the primary simulation.

If the amplitude of the periodic modulation of the Hopf parameter, A is increased from 0.1 to 0.5, the initial circle gradually changes into a cycloid-shaped form, see Fig. 2. If, instead, the frequency ω_μ is increased, the system undergoes similar changes, where, however, the frequency change is reflected in a change of the periodic structure of circumference (see Fig. 3).

As the next situation, we investigate the behavior of our Hopf oscillator when the Hopf parameter $\bar{\mu}$ is held constant, while the frequency of the input signal, ω , is changed. Figure 4 shows the simulated results when $\bar{\mu}$ is constant. From this figure, we confirm that the obtained attractor could not show complexity. In Fig. 5, the frequency of the input signal is changed from 2.1 [kHz] (bottom panel) to 2.8 [kHz] (top panel). The complex attractor can be observed around 2.4 [kHz]. We thus verified that the attractor of the Hopf oscillator model displays a pronounced complex behavior if a modulation of the control parameter $\bar{\mu}$ is implemented.

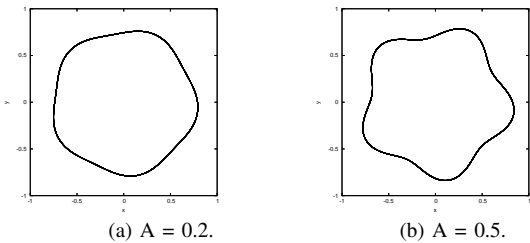


Fig. 2. Changes introduced by an increase in the amplitude A (from $A = 0.2$ to 0.5), using $\omega/(2\pi) = 2.8$ kHz and $\omega_\mu=5.0 \omega$.

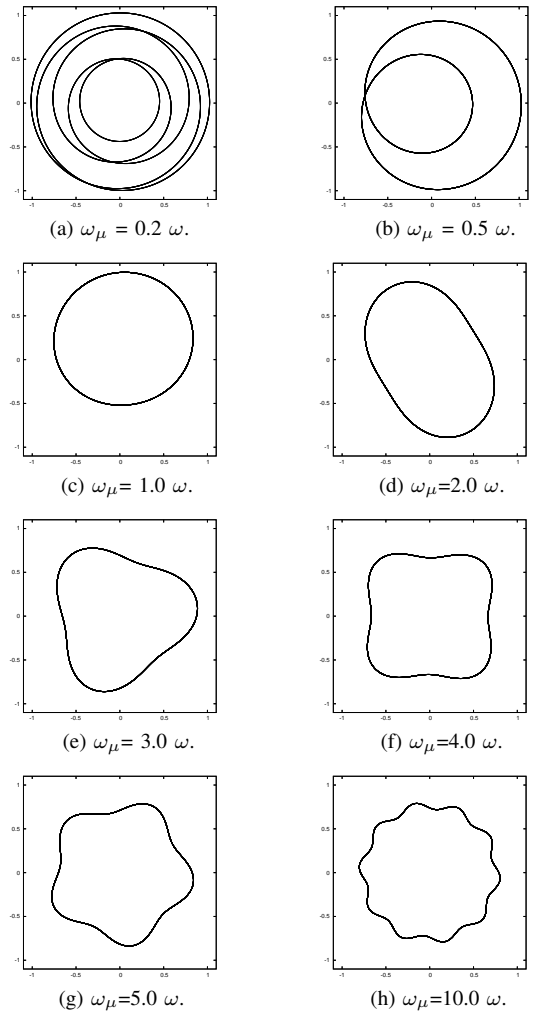


Fig. 3. Attractor of the Hopf oscillator if the frequency ω_μ of the periodically modulated Hopf parameter is increased (using $A=0.5$ and $\omega/(2\pi)=2.8$ kHz).

A. Bifurcation Diagram

In figure 6 we show the bifurcation diagram obtained when changing ω_μ . The horizontal axis is ω_μ/ω_0 and the vertical axis is x . When ω_μ/ω_0 is around 0.5, solutions of periodicity two can be observed. If ω_μ/ω_0 becomes larger than 0.85, the solutions of periodicity one appear. From this figure, we can see that this bifurcation diagram corresponds to Arnold tongues. In order to confirm this, we calculated the solutions when ω_μ and f are changed. The obtained Arnold tongues are shown in Fig. 7.

B. Lyapunov Exponent

An important confirmation of the observed dynamical behavior of the Hopf oscillator is provided by means of the Lyapunov exponent of its attractors. Figure 8 shows the calculated results of this quantity. From these results (for the non periodic solutions the Lyapunov exponents are presumably zero), it is suggestive that the corresponding complex attractors are quasiperiodic torus solutions.

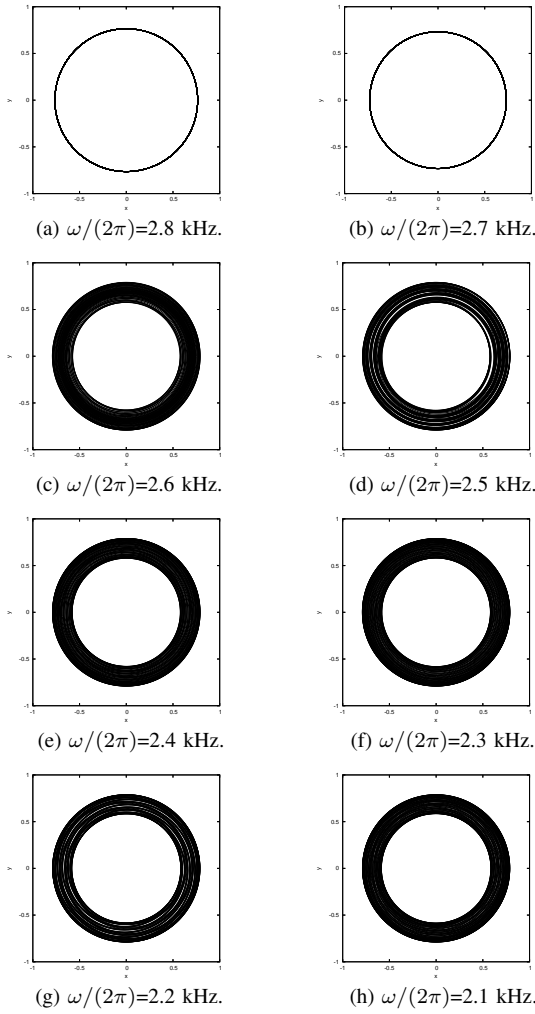


Fig. 4. Attractor of Hopf oscillator with constant $\tilde{\mu}$.

V. COUPLED HOPF OSCILLATORS

Finally, as an alternative for generating complex output by means of the previously discussed simple basic set-up, we consider Hopf oscillators coupled according to the coupling scheme shown in Fig. 9, where three Hopf oscillators are connected by ring-coupling. In this system, there are no external input forces, and the Hopf parameters μ_i , $i = 1, 2, 3$, are individually set to negative values.

The results of the obtained attractors for this set-up are shown in Fig. 10. By changing the $\tilde{\mu}$ values, again interesting changes of the attractors are observed.

VI. CONCLUSIONS

In this study, we scanned the complexity that emerges for a simple set-up involving three oscillatory frequencies, where the three frequencies either emerged from an input signal, a modulated Hopf parameter and the Hopf oscillator's own frequency, or from three different Hopf oscillators that were coupled in a ring-like fashion. A considerable richness of behaviors is observed, following the well-known paradigm of Arnold tongues and locking. In future works, we will

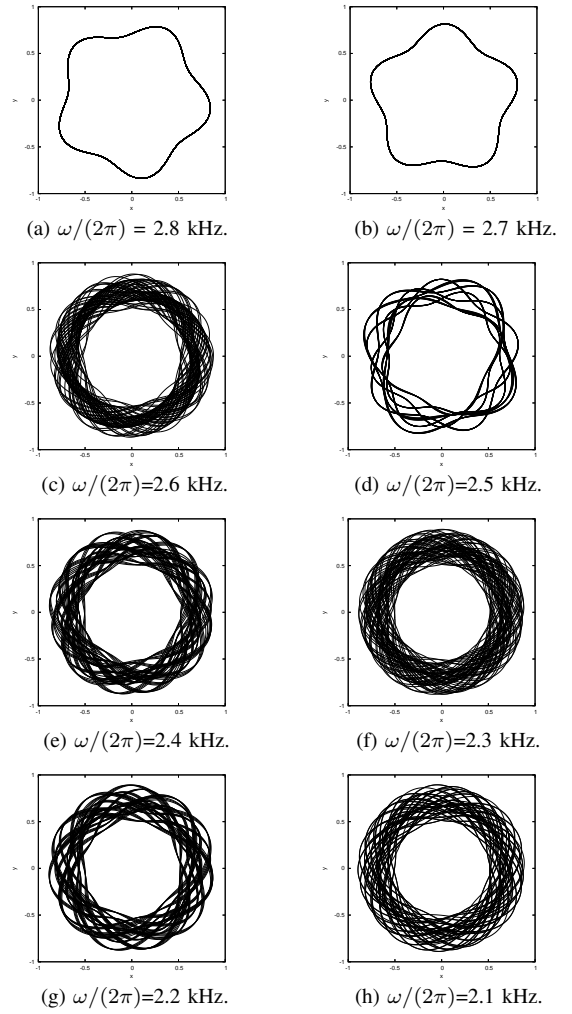


Fig. 5. Morphology of the Hopf oscillator for changing the input signal $\tilde{\mu}$ ($A=0.5$ and $\omega_\mu=5.0 \omega$).

investigate what additional features it will require for Hopf oscillators to generate stronger complex phenomena like chaos and, potentially, hyperchaos.

REFERENCES

- [1] H. Helmholtz, "Die Lehre von den Tonempfindungen als Physiologische Grundlage für die Theorie der Musik," *Vieweg, Braunschweig*, 1863.
- [2] G. von Békésy, "Experiments in Hearing," *McGraw-Hill, New York*, 1960.
- [3] E. De Boer "in The Cochlea," edited by P. Dallos, A. Popper, and R. Fay, *Springer, New York*, 1996.
- [4] T. Gold, "Hearing II. The Physical Basis of the Action of the Cochlea," *Proc. R. Soc. London B* 135, 492, 1948.
- [5] D. Kemp, "Stimulated Acoustic Emissions from within the Human Auditory System," *J. Acoust. Soc. Am.* 64, 1386, 1978.
- [6] P. Martin and A. Hudspeth, "Compressive Nonlinearity in the Hair Bundle's Active Response to Mechanical Stimulation," *Proc. Natl. Acad. Sci. U.S.A.* 98, 14386, 2004.
- [7] V. Eguiluz, M. Ospeck, Y. Choe, A. Hudspeth, and M. Magnasco, "Essential Nonlinearities in Hearing," *Phys. Rev. Lett.* 84, 5232, 2000.
- [8] A. Kern and R. Stoop, "The essential role of couplings between hearing nonlinearities," *Phys. Rev. Lett.*, 2003.
- [9] S. Martignoli, J.-J. van der Vyver, A. Kern, Y. Uwate, and R. Stoop, submitted, 2007.

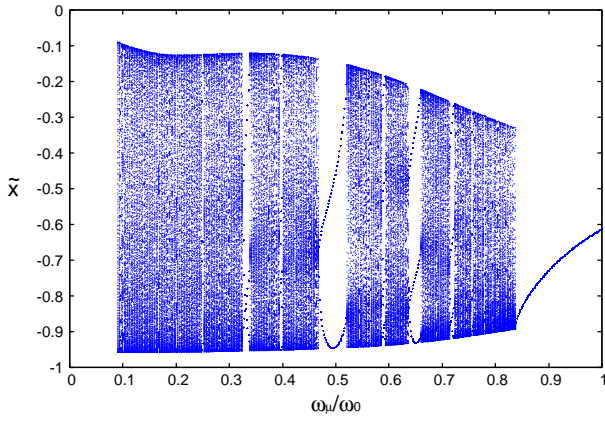


Fig. 6. Bifurcation diagram obtained by a continued frequency increase of the periodic modulation of the Hopf parameter. Order parameter is ω_μ . ω_0 is held fixed.

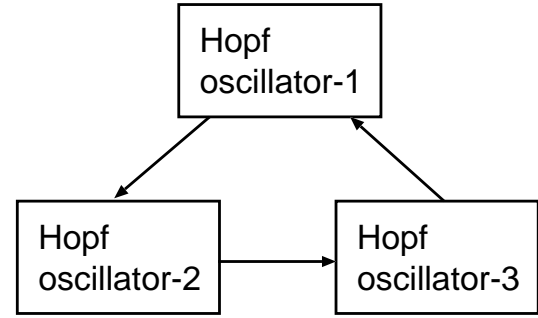


Fig. 9. Coupling scheme used for coupling three Hopf oscillators.

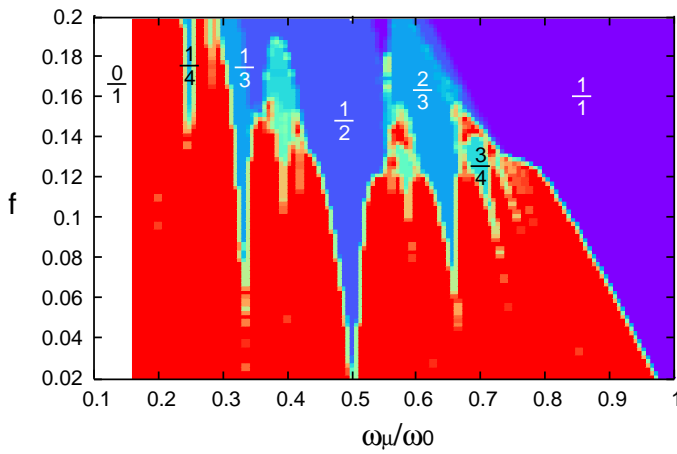


Fig. 7. Arnold tongues for the interaction via the amplitude of the input signal. $\Omega = \frac{\omega_\mu}{\omega_0}$. The inserted ratios label the periodicities associated with the respective Arnold tongues. Order parameter is ω_μ . ω_0 is held fixed.

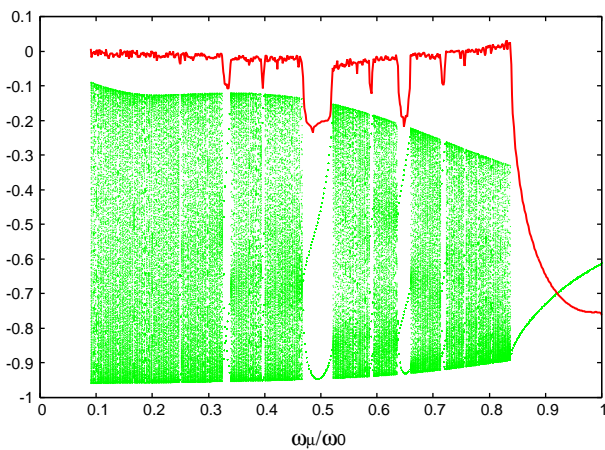
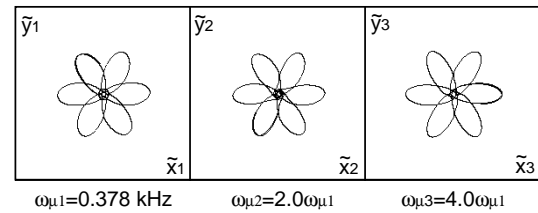
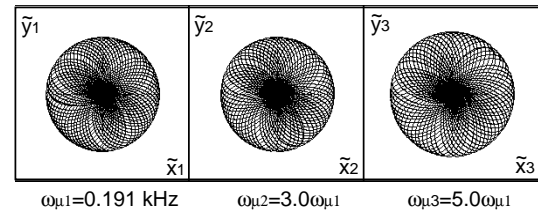


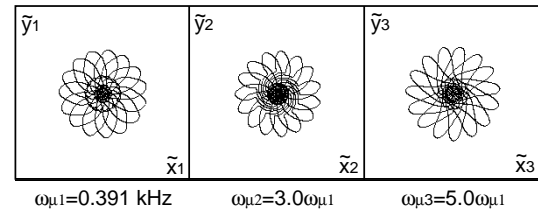
Fig. 8. Lyapunov exponents obtained in function of the order parameter ω_μ . ω_0 is held fixed.



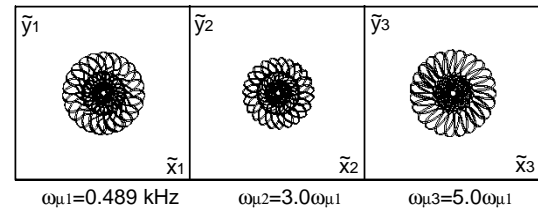
(a)



(b)



(c)



(d)

Fig. 10. Examples of attractors observed for Hopf oscillators coupled according to the scheme displayed in Fig. 9.